Determination of the Selectivity of Printed Wearable Sweat Sensors

Alicia Zörner[1], Susanne Oertel[1], Björn Schmitz[2], Nadine Lang[2],
Michael P. M. Jank[1] and Lothar Frey[1]
[1]*Fraunhofer Institute for Integrated Systems and Device Technology IISB, Schottkystr. 10, 91058 Erlangen, Germany*
[2]*Fraunhofer Institute for Integrated Circuits IIS, Am Wolfsmantel 33, 91058 Erlangen, Germany*

Keywords: Screen-printed, Biosensor, Sweat, Ammonium, Exercise, Ion-Selective Electrode, Wearable Device, Bluetooth, Selectivity, Wearable Healthcare.

Abstract: The characterization and system integration of a fully screen-printed electrolyte biosensor is described. The purpose of this sensor is to determine the state of fitness during sports activity by measuring the ammonium concentration in sweat. Focusing on the selectivity of the ammonium sensor against interfering sodium and potassium ions, the separate solution method (SSM) and the fixed interference method (FIM) are compared on the basis of a single sensing device. The latter is mainly supported by the excellent stability of the sensors. For both interfering ions, the FIM analysis shows a sufficient margin for the operation of the sensor in the desired application in wearable health and fitness monitoring from sweat. The selectivity coefficients are better than 0.01 for sodium and still better than 0.1 for potassium. SSM delivers higher selectivity in both cases, although the discrepancies in selectivity point towards further optimization potential in the sensor architecture or materials combination.

1 INTRODUCTION

In recent years, many efforts were carried out for the development of printed sensors that analyze ions in bodily fluids. In latest publications from Dam et al., (2015) and Matzeu et al., (2016), ion-selective electrodes (ISEs) are used for detection of chloride and sodium concentrations in sweat. In our previous work (Oertel et al., 2016) we already presented a printed sensor for analysis of ammonium in sweat.

The content of ammonium in sweat is correlated to physical overstrain as published by Ament et al., (1997), Alvear-Ordenes et al., (2005) and Meyer et al., (2007). Therefore, using a sensor for the direct monitoring of ammonium in sweat is very attractive for fitness as well as for healthcare applications. A combination with other body parameters, e.g. cardiovascular signals, improves the assessment of the body status in sports performance diagnostics as well as the health status for diagnostics and therapy of diseases.

The advantage of an ion-selective electrode and its main feature is the selectivity for a primary ion with respect to ions interfering from the background. For all ion-selective membranes, interfering ions that have similar size of the ionic radius and the same ionic charge could create a distracting potential at the working electrode. Therefore, it is important to determine the selectivity coefficient of the ISE.

For an ammonium-selective electrode using nonactin as ionophore, especially sodium and potassium can act as interfering ions. Both ions have the same charge as ammonium and nearly the same ionic radius. Therefore, they can affect the proper evaluation of the ammonium level. This is even more critical as both ions are main components of sweat, which are active in ranges between 25 mmol/l and 60 mmol/l for sodium and from 5 mmol/l to 18 mmol/l for potassium (Meyer et al., 2007).

For the application-oriented evaluation of the selectivity coefficient, it is very important to consider the tolerated values of the specific area of interest. Furthermore, for comparison against the results of other groups it is necessary to take into account the determination method of the selectivity coefficient (Bakker et al., 2000 and Egorov et al., 2014).

Until now, other works presenting printed ammonium-selective electrodes use only a single method for the determination of the selectivity

ZÃűrner A., Oertel S., Schmitz B., Lang N., Jank M. and Frey L.
Determination of the Selectivity of Printed Wearable Sweat Sensors.
DOI: 10.5220/0006296400810087
In *Proceedings of the 10th International Joint Conference on Biomedical Engineering Systems and Technologies (BIOSTEC 2017)*, pages 81-87
ISBN: 978-989-758-216-5

coefficient. For example, Guinovart et al., (2013) utilize the separate solution method (SSM), whereas Koncki et al., (1999) apply the fixed interference method (FIM) for the characterization of screen-printed ammonium-selective electrodes. The SSM is simple, but often is not representative for a real, i.e. containing different ions, solution. In contrast, the FIM agrees more with the experimental conditions (Spichiger-Keller, 1998), but may offer a limited range of evaluation.

In this work, we directly compare the determination of the selectivity coefficients by both respective methods and discuss the differences of the evaluation.

Measurements employing artificial sweat are conducted to evaluate the sensor in an environment close to the projected application. The data collection is based on a fully integrated electronic system transferring the derived data wirelessly to a mobile device.

In the experimental part of this paper, the fabrication of the sensor as well as the characterization methods used for determination of the selectivity of the sensor is described. Besides, the data acquisition and transfer is shortly presented. In the second part of the paper, the results of the selectivity coefficient for one sensor using both methods are shown for each interfering ion, sodium and potassium. Furthermore, first results measuring artificial sweat are presented. In the followed part the difference of the resulting selectivity coefficient are discussed.

2 EXPERIMENTS

The fabrication of the sensor using screen printing and two different methods for characterization of the sensor selectivity are described. A system for data acquisition and transfer were also developed.

2.1 Sensor Fabrication by Screen Printing

For screen-printing of the electrodes, the same process as described previously (Oertel et al., 2016) were used. However, the used screen-printed pastes were changed for optimization of the printed design. Silver-based (Loctite ECI 1006 E&C) and carbon filled (Electrodag PF-407C) pastes for screen printing were now acquired from Henkel AG & Co. KGaA (Düsseldorf, Germany). The previously used silver-silver chloride paste with a ratio of 65:35 (125-21) for the reference electrode was acquired from Creative Materials (Ayer, MA, USA). For the insulating layer, a Barium titanate (PE-BT 101) paste from Conductive Compounds was used.

The pastes were printed on flexible polyethylene naphthalate (PEN, QA65HA, 125µm, Teijin DuPont Films Japan Limited) and polyimide (PI, Kapton HN, 125µm, Müller GmbH) foils.

A stabilizing layer on top of the reference electrode (Guinovart et al., 2013) was prepared from a mixture of sodium chloride (NaCl, ≥ 99.5%, BioXtra), methanol (99.8%, anhydrous), and polyvinyl butyral (PVB, Butvar® B-98, all purchased from Sigma Aldrich).

Different mixtures of the ion-selective membrane were tested and the best result is presented. Here, the Ammonium ionophore (nonactin in Cocktail B, Fluka) was obtained from Sigma Aldrich for fabrication of the ion-selective electrode. Cocktail B consisted of the ionophore Nonactin (3.5 wt%), polyvinyl chloride (0.9 wt% PVC) as polymer matrix, tetrahydrofuran (62.3 wt% THF) as solvent, dibutyl sebacate (32.95 wt% DBS) as plasticizer, and potassium tetrakis(4-chlorophenyl)borate (0.35 wt% KTClPB) as anionic sites.

Analytical grade salts of ammonium chloride, potassium chloride, and sodium chloride were purchased from Bernd Kraft for standard calibration solutions.

The artificial sweat (1020-1-D and 1006-1-B) was purchased from synthetic urine. The composite-on of this artificial sweat corresponds to DIN ISO 9022-12 and DIN ISO 105-E04 norm and contains typical pH value of sweat and typical concentrations of sweat ingredients like urea, lactic acid, sodium and ammonium chlorides, acetic acid etc., in case of 1006-1-B, it is without ammonium chloride. We used this artificial sweat by addition a defined ammonium ion concentration of 0.1 mol/l.

For the fabrication of the sensor, an automated screen- and pattern printer from Ekra (series X1) was used. The silver-silver chloride paste was printed using a polyester screen (110 µm mesh - 34 µm wire thickness x 22.5° cover angle, 10 µm -15 µm emulsion over mesh, EOM). The other pastes, silver, carbon as well as the insulator were printed using a stainless steel screen (VA 270-0.036x22.5°, 5-10µm EOM).

The printed layers on foils were annealed at 150°C for different times (5 minutes up to 15 minutes) on a hot plate (PZ 28-2 EZ, Harry Gestigkeit). For potentiometric measurements, a 2636B Sourcemeter from Keithley instruments (Cleveland, OH, USA) was used.

The printed sensors were connected to a commercial flexible flat connector (FFC) with a pitch of 2.54 mm with seven contacts. The sensor layout was designed based on the typical pitches of commercial FFCs. The FFC was placed on a printed circuit board (PCB). The analog circuit consists of an instrumentation amplifier (G=1) and low pass filter (G=1). For data acquisition and transfer, a system on a chip (SOC) including an 8051 based low power microcontroller and RF front end is utilized. The MCU is featured by 12 bit successive approximation ADC. Data transfer is performed via Bluetooth Smart (BLE). To allow wired data transfer, an additional connector is included in the circuitry.

The data was transferred via Bluetooth Low Energy to an Android (Google, Mountain View, USA) device.

The sensor design was described in previous work by Oertel et al., (2016) and consists of a bielectrode system that combines a silver working electrode with a silver-silver chloride reference electrode. A schematic and a photograph of the sensor can be seen in Figure 1.

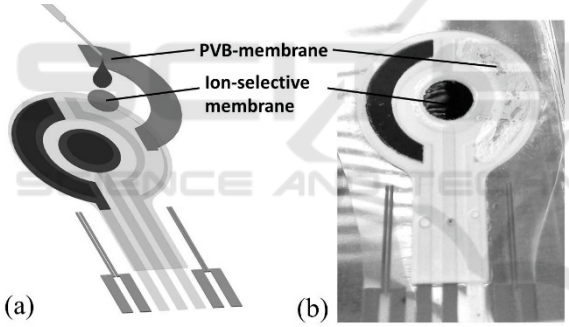

Figure 1: (a) Schematic and (b) photograph of screen-printed ammonium selective potentiometric sensor with additionally drop-casted reference and ion-selective membranes.

The sensor was printed on flexible PEN and PI foils. Moreover, the working electrode was coated with an additional carbon layer between the ion-selective membrane and the silver electrode for achieving chemical inertness. In a final printing step, an insulating layer with contact openings for electrical contacts and the active area for later deposition of the ion-selective membrane was done.

After screen-printing, the electrodes were modified (see Figure 1a). The reference electrode was covered with a mixture of PVB, methanol, and NaCl as it was published by Guinovart et al., (2013). The mixture was drop-casted and dried for about 24 hours at room temperature. Furthermore, the ion-selective membrane was produced by drop-casting a cocktail of ammonium ionophore onto the active area of the working electrode. It was again dried overnight at room temperature.

2.2 Sensor Characterization

The selectivity coefficient is derived from the response of the sensor to different ionic analytes and their respective activities. It can be calculated from the Nikolsky-Eisenman equation (Umezawa et al., 2000 and Spichiger-Keller, 1998), an extension of the Nernstian equation (Bakker et al, 2000) that considers the presence of an interfering ion:

$$\log K_{ij} = \left(E_j - E_i\right)\frac{z_i F}{2.303RT} - \frac{z_i}{z_j}\log a_j + \log a_i \quad (1)$$

with K_{ij} as the selectivity coefficient, E_j the potential of the interfering ion j, E_i the potential of the primary ion i, z_i the valency of the primary ion i, z_j the valency of the interfering ion j, R the universal gas constant, T the temperature, F the Faraday constant, a_i the activity of the primary ion i and a_j the activity of the interfering ion j.

Using the separate solution method (SSM), the calibration curves of separate standard solutions of both, the primary ion and the respective interfering ion, are prepared with varying ion activities. (Umezawa et al., 2000). In our case the concentration range of the solutions was between 10^{-5} mol/l (pC 5) and 10^{-1} mol/l (pC 1) for each of the ions, ammonium, sodium, and potassium. The range refers to the typical ammonium level in sweat before and during physical overstrain (Czarnowski et al., 1992, Guinovart et al., 2013).

The electromotive force (EMF) of the primary ion and the interfering ions were recorded successively starting from low concentrations. A current-less measurement that does not distort the output voltage is conducted applying the high-impedance voltage measurement mode of the 2636B source meter delivering 10^{14} ohms of internal resistance. Each data point was collected after 7 min of settling time. After measurement, the sensor was rinsed with deionized water and submerged into the subsequent standard solution.

For determination of the selectivity coefficient via SSM, the resulting EMFs of primary ions and interfering ions are evaluated at a certain concentration level. At equal a_i and a_j, equation 1 can be reduced to

$$K_{ij}^{SSM} = a_i^{1-\frac{z_i}{z_j}} e^{(E_j - E_i)\frac{z_i F}{2.303RT}} \quad (2)$$

For the fixed interference method (FIM) the electromotive force for solutions of constant ion activity of the interfering ion and varying activity of the primary ion is measured. For the determination of the selectivity, the EMF is plotted versus the logarithm of the ion activity of the primary ion (Umezawa et al., 2000). If the effect of the interfering ion on the sensor is dominant, typically at low concentrations of the primary ion, the latter is completely shielded, leading to a constant EMF. However, when the concentration of the primary ion is increased above a critical level, the EMF should follow the concentration of the primary ion only, leading to a linear increase of the EMF. Fitting the constant branch depicting the EMF of the interfering ion and the range, where the primary ion dominates, delivers two lines that intersect at a characteristic concentration a_i of the primary ion. This value refers to the minimum detectable concentration of the primary ion with respect to the distorted environment, i.e. the concentration a_j of the interfering ion. The respective selectivity coefficient is calculated as follows (Umezawa et al., 2000):

$$K_{ij}^{FIM} = a_i / a_j^{\frac{z_i}{z_j}} \quad (3)$$

2.3 Automated Calibration and Data Acquisition via Mobile Device

The printed sensor circuit is attached to a multifunctional electronic box.

The differential sensor voltage is converted to a ground related and filtered voltage by the analog front end. This ground related voltage is then acquired by the ADC of the MCU at a sampling rate of 2 Sa/s. To lower the power consumption for data transmission, five samples are accumulated on the MCU's RAM before sending the data via BLE to the mobile device. Thus a transmission rate of 0.4 Hz is used.

The data received by the Android mobile device can be used for further data handling and evaluation (see Figure 2). When a calibration for the sensor is available, the app calculates the corresponding concentration and visualizes a range in which the concentration lies.

For the calibration, the sensor is submerged into the different calibration solutions (pC 5 to pC 1) for 7 minutes each to get constant values over time (Oertel et al., 2016). This covers the typical ammonium range in sweat before and during physical strain.

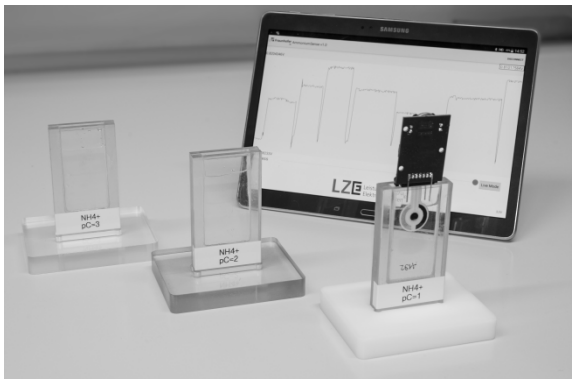

Figure 2: Sensor system with circuit board and data acquisition/transfer via Bluetooth 4.0 for the concentration of pC 3, pC 2 and pC 1.

3 RESULTS

Selectivity coefficients of the ammonium sensor were evaluated by separate solution method (SSM) and fixed interference method (FIM) for the interfering ions sodium and potassium.

3.1 Selectivity against Sodium

In Figure 3 the resulting calibration curves of the two methods are shown for sodium as disturbing ion.

In the case of SSM (Figure 3a), the EMFs for the concentrations of 0.1 mol/l (pC 1), 0.01 mol/l (pC 2) and 0.001 mol/l (pC 3) of both ions were used for calculation of the selectivity coefficient according to equation 2. The coefficient for FIM (Figure 3b) was calculated from the interpolated minimum detectable concentration of the primary ion with respect to the distorted environment. This is derived from the intersection of the previously described fits of the constant branch related to the interfering ion and the linear range, where the primary ion dominates (see dotted lines in Figure 3b).

The mean selectivity coefficient obtained from SSM $\left(K_{NH_4^+,Na^+}^{SSM}\right)$ is 0.0034 ± 0.0003. The coefficient at each concentration is also observable in Figure 3a by the inverted triangles. It is shown that the selectivity coefficient is nearly constant in this region of concentration. Selectivity coefficient determined by FIM $\left(K_{NH_4^+,Na^+}^{FIM}\right)$ is 0.0095. The coefficients are comparable to the results published by Guinovart et al., (2003, $K_{NH_4^+,Na^+}^{SSM} = 0.0013$) and Koncki et al., (1999, $K_{NH_4^+,Na^+}^{FIM} = 0.0079$).

In both measurements, the same sensor was used. Despite numerous measurements at full range of concentrations during SSM, the EMF of the constant branch in FIM (Figure 3b) is equivalent to the EMF of pC 2 of sodium measured by SSM. Therefore, no additional calibration of the sensor is necessary before FIM as there is no aging of the sensor visible. Nevertheless, the selectivity derived by FIM shows a slightly increased value with a difference of 0.0061.

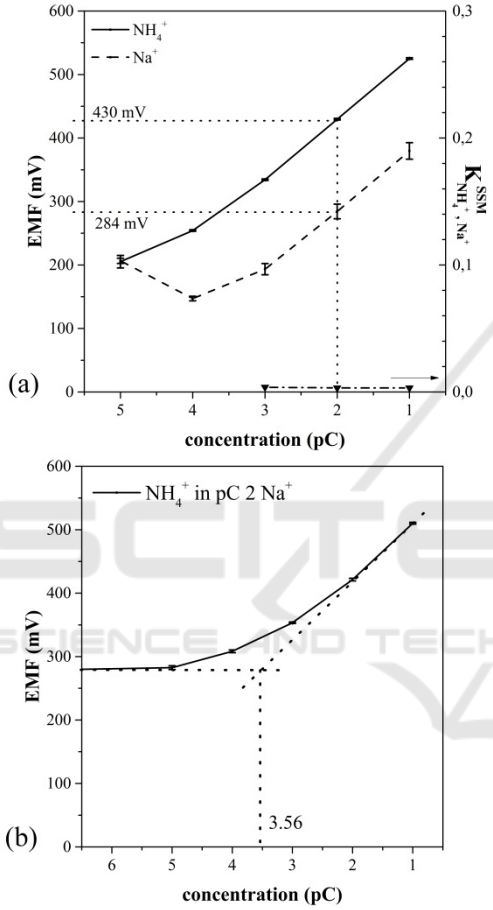

Figure 3: Measurement of ammonia concentration upon interference with sodium for the determination of the selectivity coefficients using (a) SSM and (b) FIM.

3.2 Selectivity against Potassium

For the determination of the selectivity coefficient towards potassium, the resulting calibration curves are shown in Figures 4a and b.

With respect to the measurements shown for sodium interference, the EMF values of standard solutions of potassium are closer to those for ammonium at each respective concentration. From the SSM calibration curve (Figure 4a), a reduced selectivity against potassium can be derived. This is due to the ionic radius of potassium, which is closer to that of ammonium.

The mean selectivity coefficient via SSM $\left(K^{SSM}_{NH_4^+,K^+}\right)$ is 0.0832 ± 0.0086 (see inverted triangles in Figure 4a) and is almost constant for the linear range of the concentration as it is in the case of sodium. Here, the sensor achieved a slightly increased selectivity compared to the result of Guinovart et al., (2000) obtaining a selectivity coefficient of 0.0158 using SSM.

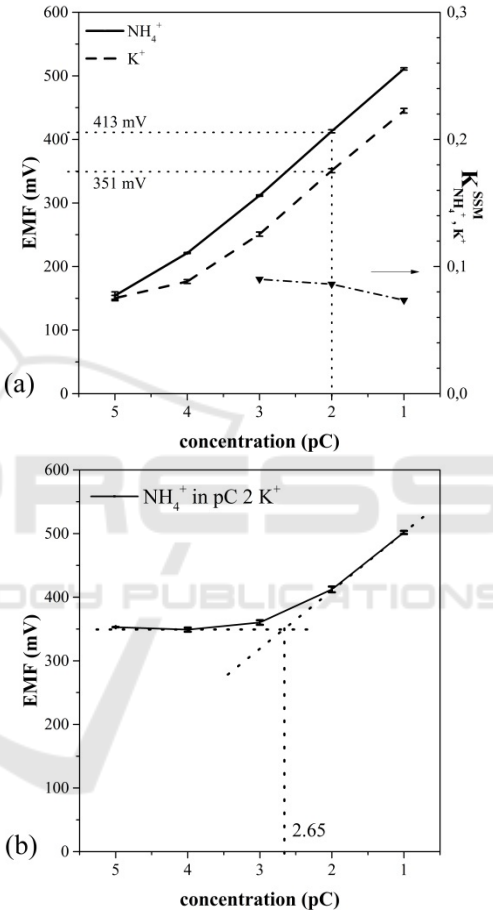

Figure 4: Calibration curves for determination of the selectivity coefficient using (a) SSM and (b) FIM for the interfering ion potassium.

Again, the EMF of the constant branch in the FIM measurement corresponds to the potassium concentration of pC 2 of the SSM calibration curve. The increased minimum detectable concentration of the primary ion (pC 2.65) is confirming the observation of a reduced selectivity coefficient derived from SSM method.

The resulting selectivity determined by FIM $\left(K^{FIM}_{NH_4^+,K^+}\right)$ is 0.0912. Again, a slightly increased

coefficient for FIM can be recognized when compared to SSM (with a difference of 0.008). Compared to the published work by Koncki et al., (1999) with a selectivity coefficient of 0.0398, our sensor achieved a slightly increased selectivity.

3.3 Artificial Sweat

Two compositions of artificial sweat were measured to test the selectivity of the sensor in more realistic environments. After recording the ammonium calibration curve, the sensor was dipped into artificial sweat with specific ammonium concentrations of 0.065 mol/l (1020-1-D) and 0.1 mol/l (1006-1-B). The measured EMF values of both artificial sweat samples as well as the EMFs of 0.065 mol/l and 0.1 mol/l ammonium standard solutions are listed in Table 1. The shift of the EMF for the ammonium standard solution compared to the calibration curves of the SSM is due to the long shelf time between the measurements. However, the slope of the calibration curve remains constant. For the measurement of the artificial sweat, a slight shift of 40 mV (1020-1-D) and 32 mV (1006-1-B) compared to ammonium standard solution is observable, which is due to the influence of the contained ions, especially the high amount of sodium as well as the influence of the pH.

Table 1: Resulted EMFs for ammonium standard solution and artificial sweat (1020-1-D and 1006-1-B).

	EMF in mV		
c in mol/l	Ammonium Standard Solution	1020-1-D	1006-1-B
0.1	422		454
0.065	400	440	

4 DISCUSSION

Compared to already published selectivity coefficients of printed ammonium-selective sensors (Guinovart et al., 2013 and Koncki et al., 1999), our fully-printed sensor shows similar selectivity and for the first time compares FIM to SSM selectivity data using same devices for both techniques.

The comparison of the selectivity coefficients determined via SSM and FIM shows for both, sodium and potassium, a higher value using FIM technique. This is contradictory to the theory, because the determination of the selectivity coefficient based on ideal Nernstian behavior should be independent on the method (Bakker et al., 2000).

However, Figures 3a and 4a already feature a non-ideal behavior expressed by an increase of the EMF that is roughly +35 mV/pC higher than the expected Nernstian slope of 59 mV in the ammonium, sodium, and potassium standard solutions. According to Bakker et al., (2000), possible reasons for this deviation can be long-term degradation of the selective membranes or electrodes or sample-to-sample variations.

The printed sensor in this work was tested over a period of a few months. The repeated measurement of calibration curves after treatment in different ion environment showed the same slope and potentials without shift within one month, so the sensors show sufficient long-term stability without aging effects. Considering the reproducibility of the calibration curve, the fabrication of sensors after three printing runs yields sensors with equivalent behavior. The sensors showed also no hysteresis in the calibrations curves of ammonium ions from low to high and from high to low concentrations. Furthermore, the utilization of a single sensor for both extraction techniques rules out sample variations in this work. Besides, further work is in progress testing the reproducibility of the sensor selectivity prepared with the same composition of the ion-selective membrane. So far, the sensors show promising results.

The stability of the reference electrode was proven by means of cyclic voltammetry (not shown here). By comparing cyclic voltammetry data of fresh and used reference electrodes, no aging of the reference electrodes could be observed.

Since most of the possible reasons for the deviant value of the Nernstian slope are already disproved, other reasons like effects caused by the solid-state multilayer construction of the sensor and enhanced diffusion of ammonium through the membrane (Nery et al., 2016) need to be analyzed in greater detail.

However, the measurement via FIM represents in general more realistic conditions when aiming at human sweat than the measurement via SSM (Spichiger-Keller, 1998).

5 CONCLUSIONS

In this work, we reported data on the selectivity of a fully-screen printed ammonium sensor for analysis of human sweat against the main interfering ions, sodium and potassium.

Within physiologically reasonable concentrations of the species under consideration, the sensor

delivers excellent selectivity against the secondary ions. The more application-related fixed-interference method (FIM) yields selectivity coefficients of 0.0095 and 0.0912 against sodium and potassium, respectively.

However, further investigations are necessary to understand the non-ideal Nernstian behavior, which is revealed by the difference of the selectivity coefficients derived from FIM and the complementary separate solution method.

Furthermore, the proper detection of ammonium activity in artificial sweat is reported giving reason for a viability of the approach even in harsh but realistic environments. These results encourage further research on the integration of sensors and read-out electronics with textiles for wearable functional sports clothing. Moreover, on body tests are of particular interest for future work. Here, considering possible motion artefacts are important.

ACKNOWLEDGEMENTS

This contribution was supported by the Bavarian Ministry of Economic Affairs and Media, Energy and Technology as a part of the Bavarian project ”Leistungszentrum Elektroniksysteme (LZE)”.

REFERENCES

Dam, V. A. T., Zevenbergen, M. A. G., van Schaijk, R. 2015. Flexible Chloride Sensor for Sweat Analysis. *Procedia Eng*., 120, 237-240.

Matzeu, G., O'Quigley, C., McNamara, E., Zuliani, C., Fay, C., Glennon, T., Diamond, D. 2016. An integrated sensing and wireless communications platform for sensing sodium in sweat. *Anal. Methods*, 8 (1), 64-71.

Oertel, S., Jank, M. P.M., Frey, L., Hofmann, C., Lang, N., Struck, M. 2016. Screen-printed biochemical sensors for detection of ammonia levels in sweat – towards integration with vital parameter monitoring sports gear. *Proceedings of the 9th International Joint Conference on Biomedical Engineering Systems and Technologies (BIOSTEC 2016)*, 1, 160-165.

Ament, W., Huizengau, J. R., Mook, G. A., Gips, C. H., Verkerke, G. J. 1997. Lactate and ammonia concentration in blood and sweat during incremental cycle ergometer exercise. *Int. J. Sports Med.*, 18, 35-39.

Alvear-Ordenes, I., Garcia-Lopez, D., De Paz, J., Gonzalez-Gallego, J. 2005. Sweat lactate, ammonia, and urea in rugby players. *Int. J. Sports Med.,* 26, 632-637.

Meyer, F., Laitano, O., Bar-Or, O., Mc Dougall, D., Heigenhauser, G. J. F. 2007. Effect of age and gender on sweat lactate and ammonia concentrations during exercise in the heat. *Braz. J. Med. Biol. Res.,* 40(1), 135-143.

Bakker, E., Pretsch, E., Bühlmann, P. 2000. Selectivity of Potentiometric Ion Sensors. *Anal. Chem*., 72(6), 1127-1133.

Egorov, V. V., Zdrachek, E. A., Nazarov, V. A. 2014. Potentiometric Selectivity Coefficients: Problems of Experimental Determination. *J. Anal. Chem.,* 69 (6), 535-541.

Guinovart, T., Bandokar, A. J., Windmiller, J. R., Andrade, F. J., Wang, J. 2013. A potentiometric tattoo sensor for monitoring ammonium in sweat. *Analyst*, 138, 7031-7038.

Koncki, R., Glab, S., Dziwulska, J., Palchetti, I., Mascini, M. 1999. Disposable strip potentiometric electrodes with solvent-polymeric ion-selective membranes fabricated using screen-printing technology. *Anal. Chim. Acta*, 385, 451-549.

Spichiger-Keller, U. E. 1998. Chemical sensors and biosensors for medical and biological applications. *Wiley-VCH.* 3-527-28855-4.

Umezawa, Y., Bühlmann, P., Umesawa, K., Thoda K., Amemiyay, S. 2000. Potentiometric selectivity coefficients of ion-selective electrodes. Part I. Inorganic cations (technical report). *Pure and Applied Chemistry*, 72 (10), 1851-2082.

Czarnowski, D., Gorski, J., Jozwiuk, J. and Boron-Kaczmarska, A. 1992. Plasma ammonia is the principal source of ammonia in sweat. *Eur. J. Appl. Physiol.,* 65, 135-137.

Nery, E. W., Kubota, L. 2016. Integrated, paper-based potentiometric electronic tongue for the analysis of beer and wine. *Anal. Chim. Acta,* 918, 60-68.